Biochimie 94 (2012) 2376–2381

Contents lists available at SciVerse ScienceDirect

Biochimie

journal homepage: www.elsevier.com/locate/biochi

Research paper

The cysteine 703 to isoleucine or histidine mutation of the oxidosqualene-lanosterol cyclase from *Saccharomyces cerevisiae* generates an iridal-type triterpenoid

Cheng-Hsiang Chang [1], Yi-Chi Chen [1], Sheng-Wei Tseng, Yuan-Ting Liu, Hao-Yu Wen, Wen-Hsuan Li, Chiao-Ying Huang, Cheng-Yu Ko, Tsai-Ting Wang, Tung-Kung Wu*

Department of Biological Science and Technology, National Chiao Tung University, 300 Hsin-Chu, Taiwan

ARTICLE INFO

Article history:
Received 16 February 2012
Accepted 7 June 2012
Available online 23 June 2012

Keywords:
Oxidosqualene-lanosterol cyclase
Site-saturated mutagenesis
Iridal
Homology modeling
Marneral synthase

ABSTRACT

The Cys703 to Ile or His mutation within *Saccharomyces cerevisiae* oxidosqualene-lanosterol cyclase ERG7 ($ERG7^{C703I/H}$) generates an unusual truncated bicyclic rearranged intermediate, (8*R*,9*R*,10*R*)-polypoda-5,13*E*,17*E*,21-tetraen-3β-ol, related to iridal-skeleton triterpenoid. Numerous oxidosqualene-cyclized truncated intermediates, including tricyclic, unrearranged tetracyclic with 17α/β exocyclic hydrocarbon side chain, rearranged tetracyclic, and chair–chair–chair tricyclic intermediates (compounds **3**–**9**), were also isolated from the $ERG7^{C703X}$ site-saturated mutations or the $ERG7^{F699T/C703I}$ double mutation, indicating the functional role of the Cys703 residue in stabilizing the bicyclic C-8 cation and the rearranged intermediate or interacting with Phe699, and opened a new avenue of engineering ERG7 for producing biological active agents.

1. Introduction

Oxidosqualene-lanosterol cyclase (OSC or ERG7) cyclizes (3*S*)-2,3-oxidosqualene (OS, **1**) to lanosterol (**2**) in mammals and fungi and some higher plants [1,2]. The intricate and yet highly stereo- and regio-specific cationic mechanism, which comprises prefolded substrate conformation, epoxide protonation and opening, four consecutive ring annulations, 1,2-shifted hydride and methyl groups migration, and final specific deprotonation, is of considerable interest both in considerations on the origin of sterol biosynthesis and protein engineering for pharmaceutical applications [3–11].

Protein engineering of enzyme active sites using site-saturated mutagenesis offers promising abilities both for studying structure–function-mechanism relationships of proteins and for creating new sequences with improved or novel properties [12–14]. We previously utilized site-saturated mutagenesis to elucidate several plasticity residues within *Saccharomyces cerevisiae* ERG7, which are critical for enzyme catalytic activity and/or product specificity/diversity [15–22]. Numerous oxidosqualene-cyclized truncated and rearranged products have been isolated and characterized. Reported mutants traverse chair–boat–chair to chair–chair–chair substrate prefolded conformation and/or affect carbocation intermediate stabilization as well as enzyme plasticity to generate single or multiple products.

On the other hand, biochemical characterizations of OSCs purified from various sources have also significantly contributed mechanistic insights into the cyclization/rearrangement cascade. For example, protein purification and chemical inactivation of the pig liver, bovine liver, *S. cerevisiae*, and *Candida albicans* OSC enzymes with sulfhydryl group specific agents suggested that at least two cysteine residues are critical for enzymatic activity, one directly involved in catalysis, with a second being not directly participating in the enzymatic activity, but may be involved in maintenance of the proper enzymatic conformation [23–26]. However, no precise determination of the locations of putative cysteine residues involved in the catalysis or conformation has been reported.

Multiple sequences alignment results showed that Cys703 of ERG7 is highly conserved among various OSCs from different species (Fig. 1). The produced homology model of ERG7, based on the X-ray structure of human OSC, revealed that Cys703 is a second-tier residue located proximal to the previously identified first-tier Phe699 residue with a distance of approximately 3.4 Å (Fig. 2) [27,28]. The combination of these observations suggested that Cys703 of ERG7 may be involved in catalysis directly or indirectly through the interaction with proximal residues located within the

* Corresponding author. Tel.: +886 3 5729287; fax: +886 3 5725700.
E-mail address: tkwmll@mail.nctu.edu.tw (T.-K. Wu).
[1] These authors contributed equally to this work.

0300-9084/$ – see front matter © 2012 Elsevier Masson SAS. All rights reserved.
http://dx.doi.org/10.1016/j.biochi.2012.06.014

Fig. 1. Multiple sequence alignment of oxidosqualene-lanosterol cyclase (OSC). The sequences shown are *Homo sapiens* OSC (HsaOSC), *Mus musculus* OSC (MmuOSC), *Rattus norvegicus* OSC (RnoOSC), *Saccharomyces cerevisiae* OSC (SceOSC), *Candida albicans* OSC (CalOSC), *Pneumocystis carinii* OSC (PcaOSC), *Cephalosporium caerulens* (CcaOSC), and *Alicyclobacillus acidocaldarius SHC* (AacSHC), respectively. The consensus sequences are boxed in black. These highlighted amino acid residues indicate the similarity of OSCs among different species.

protein's active site cavity surface, particularly Phe699. To further substantiate the functional role of the Cys703 in ERG7 catalysis and its interaction with Phe699, we performed the site-saturated mutagenesis of Cys703 and the Phe699/Cys703 double mutations, and characterized the product profiles.

2. Materials and methods

2.1. Site-saturated mutagenesis and non-saponifiable lipid extraction of ERG7^{C703}

Mutagenesis of Cys703 in the *S. cerevisiae* ERG7 wild-type gene was performed using the QuikChange site-directed mutagenesis kit (Stratagene, La Jolla, CA). The degenerate mutagenic primers for Cys703 were the following, with substitutions underlined and silent mutation italicized: ERG7C703X1: 5′-CAACCACTCTNNNG*CAATCG*AATACCCAAG-3′ and ERG7C703X2: 5′-CTTGGGTATT*CGATTG*CNNNAGAGTGGTTG-3′. The PCR reaction contains 0.8 mM each of dNTP, 100 ng of pRS314ERG7WT plasmid as template, 1X Pfu polymerase buffer, 10 μL of each primer (0.2 mM), 2.5 U of Pfu DNA polymerase and ddH_2O to the final volume of 20 μL. The reaction mixture was denatured at 95 °C for 2 min, and then run for 25 cycles of denaturizing at 95 °C for 30 s each, annealing at 52 °C for 1 min, polymerization at 68 °C for 10 min, and a final extension at 68 °C for 8 min. The mutations were confirmed by DNA sequencing and subsequently electroporated into the yeast strain TKW14 and selected for growth on SD + Ade + Lys + His + Met + Ura + hemin + G418 + Erg plates. The plasmids were then selected on SD + Ade + Lys + His + Met + Ura + hemin + G418 + 5-FOA plates for complementation of cyclase activity as described previously. Transformants were grown in SD + Ade + Lys + His + Met + Ura + hemin + G418 + Erg medium for non-saponifiable lipid (NSL) extraction and column chromatography. The NSL extract was fractionated by silica gel column chromatography and assayed by gas chromatography–mass spectrometry (GC–MS) to examine triterpenoid products with a molecular mass of m/z = 426 as described previously.

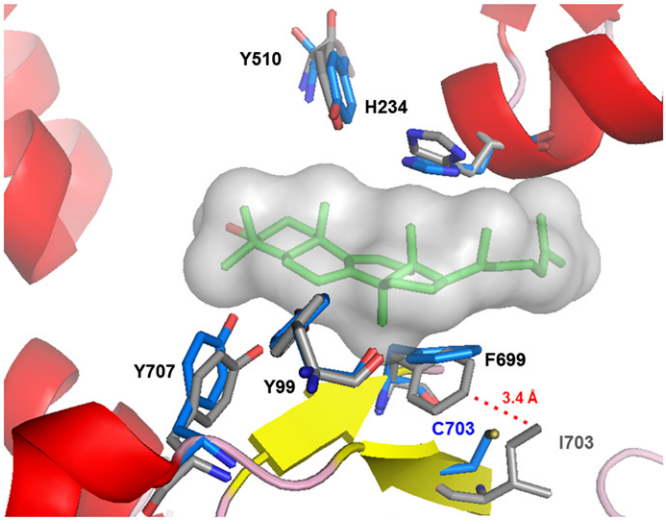

Fig. 2. The superimposed homology model of *S. cerevisiae* ERG7^{C703I} (gray) and ERG7^{WT} (blue) complexed with protosteryl C-17 cation (green). (For interpretation of the references to colour in this figure legend, the reader is referred to the web version of this article.)

2.2. Chemical shifts of (8R,9R,10R)-polypoda-5,13E,17E,21-tetraen-3β-ol

Chemical ^{1}H NMR (600 MHz, CD_2Cl_2) spectra showed distinct chemical shifts of four vinylic methyl signals (δ 1.58, s, 3 Me, Me-27, Me-28, and Me-29; δ 1.66, s, 1 Me, Me-30) with four sets of undistinguishable trivalent methine protons (δ 5.08, m, 3H, H-13, H-17, and H-21; δ 5.43, t, 1H, H-6) and four saturated methyl groups (δ 1.08, s, 1 Me; d, 1.09, s, 1 Me, Me-23, and Me-24; δ 0.84, s, 1 Me, Me-25; and δ 0.78, d, 1 Me, Me-26), as well as one methine proton attached to the carbon bearing a hydroxyl group at δ 3.42. Notably, all proton signals on the ^{1}H NMR are almost identical to the previous assignment of one bicyclic alcohol obtained from the $SnCl_4$-catalized nonenzymatic cyclization of oxidosqualene, except for some blur or ignored signals that were not previously identified [29–31]. Moreover, the spectra characteristic of one 6/6-fused bicyclic intermediate, which was isolated from a prokaryotic squalene-hopene cyclase mutant, was similarly observed in that of novel product from *S. cerevisiae* ERG7^{C703} mutants herein. The ^{13}C NMR (150 MHz, CD_2Cl_2) spectrum revealed the presence of three set of tertiary-quaternary substituted double bonds (δ_c = 124.25, 131.21; 124.42, 134.92, and 125.30, 134.47 ppm) and one set of weak tertiary-quaternary substituted double bonds at δ_c = 120.03 and 142.63 ppm, respectively.

The HSQC spectrum showed that one olefinic methine protons (δ 5.43 ppm) is attached to the carbon at 120.03 ppm whereas other three methine protons at δ 5.08 are correlated to three tertiary carbons at δ_c = 124.25, 124.42, and 125.30 ppm, further suggesting a bicyclic skeleton with a ring-fused tertiary-quaternary substituted double bond and three exocyclic olefinic double bonds at its hydrocarbon side chains. The HMQC spectrum also showed that the methylene protons at δ 2.05 (5-H), δ 1.96 (4-H), δ 1.88 (3-H) are attached to the carbons at δ_c 21.99, 26.62, 26.78, and 39.73, implying the correlation of methylene groups at exocyclic hydrocarbon side chain. For the signals within the fused ring the methine proton at δ 1.65 (H-8) is attached at the carbon at 32.81 ppm (C-8), methine at 2.1 ppm (H-10) is attached to carbon at 39.98 ppm, and methine proton at δ 3.42 is attached to the carbon at 76.56 ppm (C-3), revealed by HSQC spectrum.

Moreover, the critical connectivity of hydrocarbon side chains and relative double bond positions were observed from the HMBC spectrum, and were described as following. (1) The chemical shift of δ 5.08 revealed the connectivity with methyl groups at δ_c 15.88 (Me-27), δ_c 16.01 (Me-28), δ_c 17.66 (Me-29), and δ_c 25.67 (Me-30), as well as six methylene signals at δ_c 21.99, 26.62, 26.78, and 39.73 ppm (C-11, C-12, C-15, C-16, C-19, and C-20), respectively; The carbon at 124.25 ppm (C-21) is synchronously coupled to two methyl protons at δ 1.58 (Me-29) and 1.66 (Me-30) by ^3J connectivity, whereas carbon at 124.42 ppm (C-17) and 125.29 ppm (C-13) only showed ^3J coupling to one methyl protons of δ 1.58 (Me-27 or Me-28), respectively. Moreover, the carbon at 124.25 ppm (C-21),

and 124.42 ppm (C-17) coupled with methylene protons at δ 2.05 and δ 1.96 (H-15, H-16, H-19, or H-20) while 125.30 ppm (C-13) further displayed a ^{3}J connectivity at δ 1.88 (H-11). These observations in the HMBC spectrum clearly illustrated the exocyclic hydrocarbon side chain's connectivity. (2) The tertiary carbon at 32.81 ppm (C-8) and quaternary carbon at 35.96 ppm (C-9) exhibited their connectivity to two same methyl groups (δ 0.78, Me-26 and δ 0.84, Me-25) whereas another tertiary carbon of C-10 (39.98 ppm) only correlated to one of these two methyl groups, further suggesting the connectivity from C-8 to C-10 which is scaffold next to the exocyclic hydrocarbon side chain in the B-ring structure. (3) The methyl groups at A-ring (δ 1.08, s, Me-23; δ 1.09, Me-24) showed ^{2}J connectivity to one quaternary carbon at 42.10 ppm (C-4), ^{3}J connectivity to methine carbon bearing a hydroxyl group at 76.56 ppm (C-3), and ^{3}J connectivity to quaternary carbon at 142.63 ppm, that confirmed the position of final deprotonation for the formation of a ring-fused tertiary-quaternary substituted double bond.

Finally, the presence of NOEs among Me-25/H-8, the absence of NOEs between Me-25/H-10, and the absence of $^{1}H-^{1}H$ COSY correlation between Me-25/Me-26 confirmed the stereochemistry of the C–B 6-6 bicyclic nucleus. These findings unambiguously established the unknown compound to be (8*R*,9*R*,10*R*)-polypoda-5,13*E*,17*E*,21-tetraen-3β-ol, a chair–boat (C–B) 6-6 bicyclic product with trans–syn stereochemistry and $\Delta^{5,17,21}$ double bonds. Interestingly, the steric isomer with chair–chair conformation from the $SnCl_4$-catalized nonenzymatic cyclization of oxidosqualene exhibited the similar but slightly different spectrometric data with our unknown compound in the NMR spectrum [29–31].

3. Results and discussion

The ERG7^{C703X} site-saturated and ERG7$^{F699/C703}$ double mutations were generated, using the QuikChange site-directed mutagenesis, and transformed into a yeast TKW14 strain for genetic selection and product characterization, as previously described [16]. Following genetic selection with ergosterol complementation experiments, the non saponifable lipid (NSL) from each mutant were extracted and applied to $AgNO_3$-impregnated silica gel column for product profiles characterization, using GC–MS and NMR (^{1}H, ^{13}C NMR, DEPT, $^{1}H-^{1}H$ COSY, HMQC, HSQC, HMBC, and NOE)spectroscopic techniques.

Table 1 shows the genetic selection results and the product profiles of the ERG7^{C703X} site-saturated and ERG7$^{F699/C703}$ double mutants with molecular mass of 426 Da. Neither lanosterol nor truncated intermediates could be detected from the non-viable ERG7^{C703X} (X = A/L/F/Y/W/E/P/R/K/Q/M) mutants which is consistent with the genetic selection results. The ERG7^{C703D} and ERG7^{C703N} viable mutants produced **2** as the sole product. Both ERG7^{C703I} and ERG7^{C703H} produced a new yet unidentified compound with a $C_{30}H_{50}O$ formula, in conjunction with **2**, (13α*H*)-isomalabarica-14(26),17*E*,21-trien-3β-ol (**3**), (13α*H*)-isomalabarica-14*E*,17*E*,21-dien-3β-ol (**4**), (13α*H*)-isomalabarica-14*Z*,17*E*,21-dien-3β-ol (**5**), protosta-13(17),24-dien-3β-ol (**6**), (13α*H*)-malabarica-14*E*,17*E*,21-trien-3β-ol (**8**), and 17α-protosta-20(22),24-dien-3β-ol (**9**), by comparison with authentic standards by ^{1}H and ^{13}C NMR as well as GC–MS [15–22]. The new compound was isolated and further characterized with NMR and demonstrated to be (8*R*,9*R*,10*R*)-polypoda-5,13*E*,17*E*,21-tetraen-3β-ol (**10**) (Fig. 3). Interestingly, compound **10** showed the same relative stereochemistry as observed in 10-deoxy-17-hydroxyiridal, an iridal-skeleton triterpenoid [29–32]. The ERG7^{C703X} (X = G/V/T) mutants produced **2** and **3**,while the ERG7^{C703S} mutant produced **2**, **3** and protosta-16,24-dien-3β-ol (**7**). The ERG7^{C703I} mutant produced diverse product profile **2**, **3**, **5**, **6**, **8**, **9**, and **10** in the relative ratio of 20:22:11:10:15:18:4. The ERG7^{C703H} mutant produced diverse product profiles, including **2**, **3**, **4**, **5**, **6**, **9**, and **10**, in the ratio of 47:12:3:3:3:31:1. The non-viable genetic selection and no product formation results of many ERG7^{C703X} (X = A/L/F/Y/W/E/P/R/K/Q/M) mutants indicated a possible functional role of Cys703 in ERG7 catalysis. The catalytic competency of ERG7^{C703X} (X = G/V/T/I/S/H) mutants to lanosterol production indicated that Cys703 is not directly involved in catalysis. Further identification of diverse product profile produced by the ERG7$^{C703S/I/H}$ mutants may suggest an indirect functional role of Cys703, presumably interacts with spatially proximal residues such as Phe699.

To investigate the interaction between Cys703 and Phe699 of ERG7, the ERG7$^{F699A/C703I}$, ERG7$^{F699T/C703I}$, and ERG7$^{F699M/C703I}$ double mutations were performed. Previous studies uncovered Phe699 as an essential residue involved in catalysis. Product profile analysis of the ERG7^{F699X} mutants also showed that the F699A mutation did not produce any product, whereas the F699T, and F699M mutations produced a single and a diverse product profile, respectively [21]. In the present study, genetic selection and product profile characterization results showed that the ERG7$^{F699A/C703I}$ double mutant caused yeast non-viability and no product formation, as expected. Alternatively, the ERG7$^{F699T/C703I}$ double mutant altered product specificity from a single compound **6** (>99.8%) to multiple products **2**, **6**, and protosta-20(22),24-dien-3β-ol (**11**) in the relative ratio of 15:67:13. The ERG7$^{F699M/C703I}$ double mutant completely abolished both the enzymatic activity and product formation. In parallel, steady-state kinetic analysis also revealed that the ERG7$^{F699T/C703I}$ double mutant exhibited a 12-fold decrease in the V_{max}/K_M value but only with a slight change in the binding affinity for the substrate. Decline of the V_{max}/K_M value could be attributed to the mutual interaction between Cys703 and

Table 1
The product profiles of *S. cerevisiae* ERG7^{C703X} site-saturated and ERG7$^{F699A,T,M/C703I}$ double mutants.

AA substitution	2	3	4	5	6	7	8	9	10	11
C703	100									
C703I	20	22		11	10		15	18	4	
C703H	47	12	3	3	3			31	1	
C703S	89	5				6				
C703V	97	3								
C703T	96	4								
C703G	91	9								
C703D	100									
C703N	100									
F699A/C703I	No product									
F699T/C703I	15				67					13
F699M/C703I	No product									

[a]Neither cell viability nor product was characterized for the rest of the ERG7^{C703X} mutants.

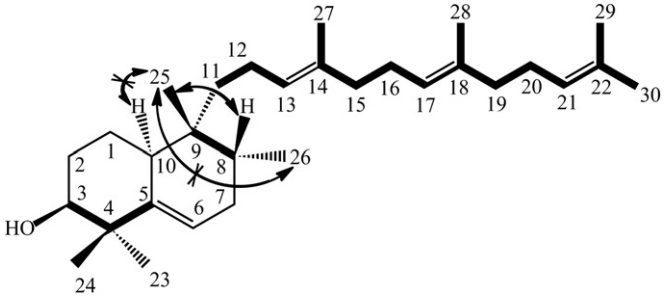

Fig. 3. Bond connectivity and stereochemistry established by HSQC/HMBC (bold bond, –) and NOE interaction (curved arrows) of (8*R*,9*R*,10*R*)-polypoda-5,13*E*,17*E*,21-tetraen-3β-ol.

Phe699 residues that introduction of the Cys703 mutation at the pre-existed Phe699 mutant further affected enzymatic conformation and the interaction between Phe699 and the cationic intermediate. This in turn affected the reaction rate and shifted the product profile from a single product to diverse products and from diverse products to no product formation.

A likely mechanism for the ERG7^{C703X} mutants that leads to diverse product profiles is shown in Scheme 1. The unusual structural features of **10** can be rationalized via a series of methyl and hydride shifts starting from a bicyclic C-8 carbocation intermediate (**I**, lanosterol numbering). In the ERG7^{C703I} mutant, **OS** is folded in either a chair–boat–chair (C–B–C) or a chair–chair–chair (C–C–C) conformation. Most of the C–B–C substrate conformers are cyclized to a C–B–C 6-6-5 tricyclic Markonikov C-14 cation **IIa**, that is followed either by direct abstraction of a proton from C-26 or C-15 to yield **3**, **4**, or **5** as end product, or by C-ring expansion and subsequent D-ring annulation to generate the protosteryl C-20 cation (**III**) with different stereochemical control at the C-17 position (**IVa** and **IVb**). Alternatively, minor amount of the C–B–C substrate conformer undergoes cationic cyclization to the C-8 cation **I** and then consecutively migrates a hydride from H-9β → H-8β, a methyl-group from Me-10β → Me-9β, and another hydride from H-5α → H-10α to generate a bicyclic C-5 cation **Ia**, which then loses a proton from C-6 to form compound **10**. Notably, the cation **IVa** with a 17α-exocyclic hydrocarbon side chain undergoes deprotonation from H-22 to produce **9**; whereas the cation **IVb** with a 17β-exocyclic hydrocarbon side chain proceeds with a backbone rearrangement of H-17α to H-20α to generate the protosteryl C-17 cation **V**. Elimination of a proton at C-13 and C-16 yielded **6** and **7**, respectively. Subsequent skeletal rearrangements of two hydride shifts (H-13α → H-17α and H-9β → H-8β) and two methyl groups (Me-14β → Me-13β and Me-8α → Me-14α) generate the lanosteryl C-8/C-9 cation (**VI**), which undergoes deprotonation at C-9 or C-8 to form **2**. Alternatively, the C–C–C substrate conformer is cyclized to a C–C 6-6-5 tricyclic C-14 cation **IIb**, that is followed by direct abstraction of a proton from C-15 to yield **8** as the end product.

Iridal-type compounds are biogenetically interesting mono-, bi-, or spiro-cyclic triterpenoids discovered first by Marner et al. [32]. They exhibit a variety of biological activities, including cytotoxicity, PKC activation, RasGRP pathway modulation, and ichthyotoxic activity [33–38]. The biosynthesis of iridal-type triterpenoids has been hypothesized to derive from oxidosqualene cyclization via a B-ring boat intermediate [29–32]. Recently, Xiong et al. isolated a marneral synthase (MRN1) from *Arabidopsis thaliana* that catalyzes the formation of an iridal skeleton triterpenoid and validated the abovementioned hypothesis [39]. In the present study, we identified the ERG7^{C703I} and ERG7^{C703H} mutants that can catalyze the biosynthesis of truncated bicyclic rearranged intermediate related to iridal triterpenoids, further supporting the evolutionary relationships between marneral synthase and oxidosqualene cyclases. Interestingly, MRN1 contains methionine in place of cysteine at the corresponding position. Previously, we identified the adjacent first-tier residue Phe699 and showed its functional role in affecting substrate folding, C- and D-ring annulation, and exocyclic side chain stereochemistry [17,21]. Consistent with the observation is the deletion of a single residue in this region of squalene-hopene cyclase led to incomplete cyclization with some stereochemical inversion [40]. Thus, the substitution of Cys703 with Ile or His may affect the interaction between Phe699 and **OS** to form rings C and D, resulting in the isolation of intermediate arrested at bicyclic stage for subsequent 1,2-shifts of hydride or methyl group to form the C-5 cation **Ia** and subsequent abstraction of a proton from C-6 to form compound **10**.

The homology model of ERG7 also provides some insight into the relationships between enzyme structure and product

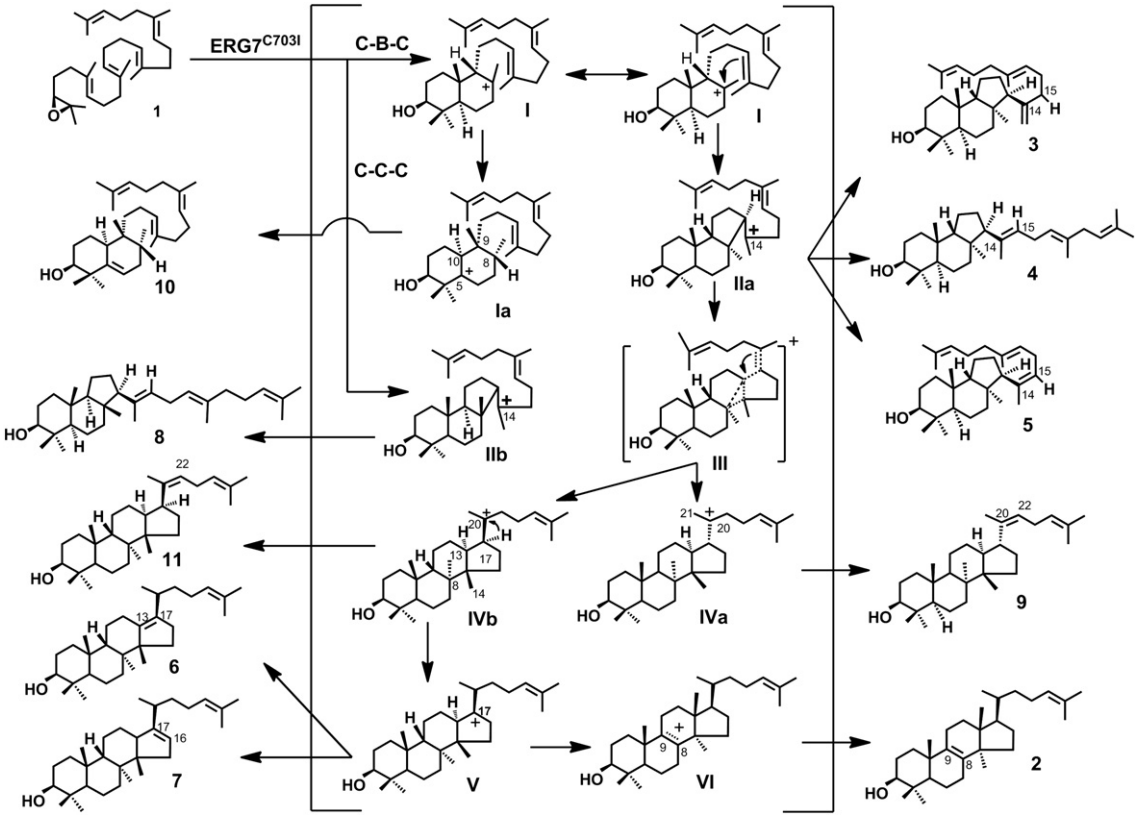

Scheme 1. The proposed cyclization/rearrangement pathways of oxidosqualene within *S. cerevisiae* ERG7^{C703I} mutant.

specificity. The homology model showed that the Phe699 is the first-tier residue with a distance of ~4.8 Å to the C-17 protosteryl cation, whereas the Cys703 is a second-tier residue located proximal to the first-tier Phe699 residue with a distance of approximately 3.4 Å [17,21]. The functional role of Phe699 has been suggested to be involved both in restricting the C–B–C conformation and/or side chain rotation as well as in stabilizing the protosteryl C-17 cation, through interaction with Tyr99, His234, and Tyr707. Substitution of Cys703 with steric Phe, Tyr, or Trp caused a steric hindrance in the active site cavity. This in turn affected the folding of the substrate and resulted in non-viable genetic selection and no product formation. Alternatively, the Cys703Ile and Cys703His mutations might partially disrupt the stabilization of Phe699 to the substrate folding or protosteryl C-17 cation, which resulted in accumulation of C–C–C or C–B–C conformer-induced tricyclic, stereochemically inverted tetracyclic, and truncated rearranged bicyclic products. Finally, the simultaneous mutation of Phe699 and Cys703 to Thr and Ile, respectively, resulted in an increase of distance between amino acid position 699 and C-17 protosteryl cation of ~0.7 Å, changing from 4.8 Å to about 5.5 Å. Consistent with the results is the observation of the decline of the reaction rate and the shift of product profile from a single product to diverse products and from diverse products to no product formation. However, exact contributions of the mutations on the product profile and proportions remain unclear and await for X-ray structure determination of the mutated proteins.

In summary, this is the first example that a single amino acid mutation within ERG7 can generate a bicyclic rearranged intermediate related to the precursor of iridal triterpenoids. Furthermore, genetic selection and product characterization of the Cys703 site-saturated and Cys703/Phe699 double mutations indicated that the functional roles of the $ERG7^{C703}$ residue is involved in interactions with Phe699 or other adjacent residues to affect proper enzymatic conformation and subsequent regulation of product profile. Therefore, our results exemplify the power of protein engineering to generate a diverse product profile, which could be customized via subtle changes to the interaction between neighboring amino acid residues surrounding the active site cavity. Although the yield for the iridal-type truncated intermediate is still poor, the $ERG7^{C703I}$ mutant serves as a template for further product specificity improvement. Further studies should focus on the elucidation and engineering of new residues that directs iridal-type structures with improved product specificity.

Acknowledgments

We are grateful to Dr. John H. Griffin and Prof. Tahsin J. Chow for helpful advice. We thank the Ministry of Education, Aiming for Top University Plan (MOE ATU Plan), and the National Chiao Tung University for financial support. This work was also supported in part by the National Science Council of the Republic of China under Contract No. NSC-99-2113-M-009-008-MY3, and NSC-99-2113-M-009-004-MY2. We also thank the National Center for High-Performance Computing for running Gaussian jobs.

Appendix A. Supplementary material

Supplementary data related to this article can be found online at http://dx.doi.org/10.1016/j.biochi.2012.06.014.

References

[1] I. Abe, M. Rohmer, G.D. Prestwich, Enzymatic cycilzation of squalene and oxidosqualene to sterols and triterpenes, Chem. Rev. 93 (1993) 2189–2206.
[2] K.U. Wendt, G.E. Schulz, E.J. Corey, D.R. Liu, Enzyme mechanisms for polycyclic triterpene formation, Angew. Chem. Int. Ed. 39 (2000) 2812–2833.
[3] R. Xu, G.C. Fazio, S.P.T. Matsuda, On the origins of triterpenoid skeletal diversity, Phytochemistry 65 (2004) 261–291.
[4] I. Abe, Enzymatic synthesis of cyclic triterpenes, Nat. Prod. Rep. 24 (2007) 1311–1331.
[5] C.J. Buntel, J.H. Griffin, Nucleotide and deduced amino acid sequences of the oxidosqualene cyclase from *Candida albicans*, J. Am. Chem. Soc. 114 (1992) 9711–9713.
[6] Z. Shi, C.J. Buntel, J.H. Griffin, Isolation and characterization of the gene encoding 2,3-oxidosqualene-lanosterol cyclase from *Saccharomyces cerevisiae*, Proc. Natl. Acad. Sci. U. S. A. 91 (1994) 7370–7374.
[7] T. Hoshino, T. Sato, Squalene-hopenecyclase: catalytic mechanism and substrate recognition, Chem. Commun. (2002) 291–301.
[8] B.A. Hess, Concomitant C-ring expansion and D-ring formation in lanosterol biosynthesis from squalene without violation of Markovnikov's rule, J. Am. Chem. Soc. 124 (2002) 10286–10287.
[9] E.J. Corey, S.C. Virgil, H. Cheng, C.H. Baker, S.P.T. Matsuda, V. Singh, S. Sarshar, New insights regarding the cyclization pathway for sterol biosynthesis from (S)-2,3-oxidosqualene, J. Am. Chem. Soc. 117 (1995) 11819–11820.
[10] E.J. Corey, H. Cheng, C.H. Baker, S.P.T. Matsuda, D. Li, X. Song, Studies on the substrate binding segments and catalytic action of lanosterol synthase. Affinity labeling with carbocations derived from mechanism-based analogs of 2,3-oxidosqualene and site-directed mutagenesis probes, J. Am. Chem. Soc. 119 (1997) 1289–1296.
[11] S. Lodeiro, Q. Xiong, W.K. Wilson, M.D. Kolesnikova, C.S. Onak, S.P.T. Matsuda, An oxidosqualene cyclase makes numerous products by diverse mechanisms: a challenge to prevailing concepts of triterpene biosynthesis, J. Am. Chem. Soc. 129 (2007) 11213–11222.
[12] C. Jäckel, P. Kast, D. Hilvert, Protein design by directed evolution, Annu. Rev. Biophys. 37 (2008) 153–173.
[13] J.A. Gerlt, P.C. Babbitt, Enzyme (re)design: lessons from natural evolution and computation, Curr. Opin. Chem. Biol. 13 (2009) 10–18.
[14] P.A. Romero, F.H. Arnold, Exploring protein fitness landscapes by directed evolution, Nat. Rev. Mol. Cell Biol. 10 (2009) 866–876.
[15] T.K. Wu, Y.T. Liu, C.H. Chang, Histidine residue at position 234 of oxidosqualene-lanosterol cyclase from *Saccharomyces cerevisiae* simultaneously influences cyclization, rearrangement, and deprotonation reactions, ChemBioChem 6 (2005) 1177–1181.
[16] T.K. Wu, Y.T. Liu, C.H. Chang, M.T. Yu, H.J. Wang, Site-saturated mutagenesis of histidine 234 of *Saccharomyces cerevisiae* oxidosqualene-lanosterol cyclase demonstrates dual functions in cyclization and rearrangement reactions, J. Am. Chem. Soc. 128 (2006) 6414–6419.
[17] T.K. Wu, H.Y. Wen, C.H. Chang, Y.T. Liu, Protein plasticity: a single amino acid substitution in the *Saccharomyces cerevisiae* oxidosqualene-lanosterol cyclase generates protosta-13(17),24-dien-3β-ol, a rearrangement product, Org. Lett. 10 (2008) 2529–2532.
[18] T.K. Wu, T.T. Wang, C.H. Chang, Y.T. Liu, Importance of *Saccharomyces cerevisiae* oxidosqualene-lanosterol cyclase tyrosine 707 residue for chair-boat bicyclic ring formation and deprotonation reactions, Org. Lett. 10 (2008) 4959–4962.
[19] T.K. Wu, C.H. Chang, Y.T. Liu, T.T. Wang, *Saccharomyces cerevisiae* oxidosqualene-lanosterol cyclase: a chemistry–biology interdisciplinary study of the protein's structure–function-mechanism relationships, Chem. Rec. 8 (2008) 302–325.
[20] T.K. Wu, W.H. Li, C.H. Chang, H.Y. Wen, Y.T. Liu, Y.C. Chang, Tyrosine 99 of *Saccharomyces cerevisiae* oxidosqualene-lanosterol cyclase influences tricyclic terpenoid moiety formation with differential stereochemical control, Eur. J. Org. Chem. (2009) 5731–5737.
[21] T.K. Wu, C.H. Chang, H.Y. Wen, Y.T. Liu, W.H. Li, T.T. Wang, W.S. Shie, Alteration of the substrate's prefolded conformation and cyclization stereochemistry of oxidosqualene-lanosterol cyclase of *Saccharomyces cerevisiae* by substitution at phenylalanine 699, Org. Lett. 12 (2010) 500–503.
[22] T.K. Wu, Y.C. Chang, Y.T. Liu, C.H. Chang, H.Y. Wen, W.H. Li, W.S. Shie, Mutation of isoleucine 705 of the oxidosqualene-lanosterol cyclase from *Saccharomyces cerevisiae* affects lanosterol's C/D-ring cyclization and 17α/β-exocyclic side chain stereochemistry, Org. Biomol. Chem. 9 (2011) 1092–1097.
[23] A. Duriatti, F. Schuber, Partial purification of 2,3-oxidosqualene-lanosterol cyclase from hog-liver. Evidence for a functional thiol residue, Biochem. Biophys. Res. Commun. 151 (1988) 1378–1385.
[24] G. Balliano, G. Grosa, P. Milla, F. Viola, L. Cattel, 3-Carboxy-4-nitrophenyldithio-1,1′,2-trisnorsqualene: a site-directed inactivator of yeast oxidosqualene cyclase, Lipids 28 (1993) 903–906.
[25] L. Carrano, M. Noe, G. Grosa, P. Milla, M. Denaro, K. Islam, Solubilization and identification of essential functional groups of *Candida albicans* oxidosqualene cyclase, J. Med. Vet. Mycol. 33 (1995) 53–58.
[26] T.K. Wu, C.Y. Huang, C.Y. Ko, C.H. Chang, Y.J. Chen, H.K. Liao, Purification, tandem mass characterization, and inhibition studies of oxidosqualene-lanosterol cyclase enzyme from bovine liver, Arch. Biochem. Biophys. 421 (2004) 42–53.
[27] R. Thoma, T. Schulz-Gasch, B. D'Arcy, J. Benz, J. Aebi, H. Dehmlow, M. Hennig, M. Stihle, A. Ruf, Insight into steroid scaffold formation from the structure of human oxidosqualene cyclase, Nature 432 (2004) 118–122.

[28] K.U. Wendt, Enzyme mechanisms for triterpene cyclization: new pieces of the puzzle, Angew. Chem. Int. Ed. 44 (2005) 3966–3971.
[29] K.B. Sharpless, E.E. van Tamelen, Terpene terminal epoxides. skeletal rearrangement accompanying bicyclization of squalene 2,3-oxide, J. Am. Chem. Soc. 91 (1969) 1848–1849.
[30] F.J. Marner, I. Longerich, Isolation and structure determination of new iridals from *Iris sibirica* and *Iris versicolor*, Liebigs Ann. Chem. (1992) 169–172.
[31] F.J. Marner, T. Kasel, Biomimetic synthesis of the iridal skeleton, J. Nat. Prod. 58 (1995) 319–323.
[32] F.J. Marner, W. Krick, B. Gellrich, L. Jaenicke, W. Winter, Irigermanal and iridogermanal: two new triterpenoids from rhizomes of *Iris germanica* L, J. Org. Chem. 47 (1982) 2531–2536.
[33] J.P. Bonfils, F. Pinguet, S. Culine, Y. Sauvaire, Cytotoxicity of iridals, triterpenoids from Iris, on human tumor cell lines A2780 and K562, Planta Med. 67 (2001) 79–81.
[34] K. Takahashi, S. Suzuki, Y. Hano, T. Nomura, Protein kinase C activation by iridal type triterpenoids, Biol. Pharm. Bull. 25 (2002) 432–436.
[35] L. Shao, N.E. Lewin, P.S. Lorenzo, Z. Hu, I.J. Enyedy, S.H. Garfield, J.C. Stone, F.J. Marner, P.M. Blumberg, S. Wang, Iridals are a novel class of ligands for phorbol ester receptors with modest selectivity for the RasGRP receptor subfamily, J. Med. Chem. 44 (2001) 3872–3880.
[36] H. Ito, S. Onoue, Y. Miyake, T. Yoshida, Iridal-type triterpenoids with ichthyotoxic activity from *Belamcanda chinensis*, J. Nat. Prod. 62 (1999) 89–93.
[37] A. Corbu, G. Gauron, J.M. Castro, M. Dakir, S. Arseniyadis, A domino-based approach toward stereodefined heavily functionalized cyclohexanes: synthesis of iridal's core structure, Org. Lett. 9 (2007) 4745–4748.
[38] Z.J. Song, X.M. Xu, W.L. Deng, S.L. Peng, L.S. Ding, H.H. Xu, A new dimeric iridal triterpenoid from *Belamcanda chinensis* with significant molluscicide activity, Org. Lett. 13 (2011) 462–465.
[39] Q. Xiong, W.K. Wilson, S.P.T. Matsuda, An *Arabidopsis* oxidosqualene cyclase catalyzes iridal skeleton formation by Grob fragmentation, Angew. Chem. Int. Ed. Engl. 45 (2006) 1285–1288.
[40] T. Hoshino, K. Shimizu, T. Sato, Deletion of the Gly600 residue of *Alicyclobacillus acidocaldarius* squalene cyclase alters the substrate specificity into that of the eukaryotic-type cyclase specific to (3S)-2,3-oxidosqualene, Angew. Chem. Int. Ed. 43 (2004) 6700–6703.